

TUNE MEASUREMENTS

M. Serio

INFN - LNF - C.P. 13 , 00044 Frascati (Roma) - Italy

ABSTRACT

In this paper the concept of betatron tune and the techniques to measure it are discussed. The smooth approximation is introduced along with the terminology of betatron oscillations, phase advance and tune. Single particle and beam spectra in the presence of synchro-betatron oscillations are treated with emphasis on the consequences of sampling the beam position. After a general presentation of various kinds of beam position monitors and transverse kickers, the time domain and frequency domain analysis of the beam response to a transverse excitation are discussed and several methods and applications of the tune measurements are listed.

INTRODUCTION

The aim of this paper is to introduce the concept of betatron tune and the techniques to measure it. The subject is vast, and it is not possible to cover here all the subtleties it entails; moreover there are many substantial differences between various machines, related to size, type of particle accelerated and user requirements. Therefore we have chosen to point out general concepts and cite references whereby separate arguments are treated in a more detailed way.

In Section 1, after introducing the concept and the terminology of betatron oscillation, phase advance and tune, we introduce the smooth approximation with an example.

Single particle and beam spectra in the presence of synchro-betatron oscillations and chromaticity are treated in Section 2 with particular emphasis on the consequences of sampling the beam position. The Schottky noise associated with the beam current is also introduced.

In Section 3 we describe various types of beam position monitors and kickers and illustrate the underlying principle of operation and peculiarities.

In analogy to the study of the response of linear circuits in electronics, the equivalence of time-domain and frequency-domain analysis of beam response is outlined in Section 4, where the concept of Beam Transfer Function and its use is introduced, and other indirect methods are mentioned.

Finally we list several applications and motivations of the tune measurement.

Throughout the text the symbols ω and Ω denote *angular* frequency [$rad \cdot sec^{-1}$], while the symbol f denotes frequency [sec^{-1}].

1. BETATRON OSCILLATIONS

To introduce in a consistent way the concept of betatron tune, it is convenient to briefly review the basics of the theory of betatron oscillations. This subject has been treated rigorously and extensively by several authors [1-3] to whom the interested reader is referred.

The ideal closed path followed by a charged particle in a synchrotron or a storage ring is determined by the bending action of the magnets. The value of the magnetic field and the radius of curvature set the nominal value of the momentum.

Quadrupole lenses are arranged and powered in such a way as to provide focusing to particles deviating from the ideal closed orbit, so that the overall motion is stable, oscillating around the ideal orbit. Additional focusing in the horizontal plane can be obtained by suitably shaping the pole-pieces of the bending magnets.

The pseudo-harmonic motion of a particle with no energy error with respect to the nominal value is governed by the Hill equation

$$\frac{d^2 z}{ds^2} + K(s) z = 0 \quad , \quad (1.1)$$

where z is the generic horizontal or vertical transverse displacement from the design orbit, s is the longitudinal coordinate and $K(s)$ is a piece-wise constant focusing function satisfying the periodicity condition $K(s) = K(s + L)$. L is the machine period, i.e. the total length of the machine or a sub-multiple thereof, according to the machine symmetry.

The solution of the differential equation (1.1) is the *betatron oscillation*

$$z(s) = \sqrt{\varepsilon} \sqrt{\beta(s)} \cos [\mu(s) - \phi_0] \quad , \quad (1.2)$$

where ϕ_0 and, in the absence of damping, ε are constants of motion determined by the initial conditions, and the *betatron function* $\beta(s)$ is the positive-definite periodic solution of the differential equation (primes denote differentiation with respect to s)

$$\frac{\beta\beta''}{2} - \frac{(\beta')^2}{4} + K(s)\beta^2 = 1 \quad .$$

The phase advance $\mu(s)$ in (1.2) is defined as

$$\mu(s) = \int_0^s \frac{d\sigma}{\beta(\sigma)} \quad . \quad (1.3)$$

The *betatron tune* Q of the machine (often symbolized by ν in the American literature) is the subject of this paper. It is defined as the number of betatron oscillations in going around one machine's revolution. The total phase advance is then

$$\int_s^{s+2\pi R} \frac{d\sigma}{\beta(\sigma)} = 2\pi Q \quad , \quad (1.4)$$

where R is the average radius of curvature of the machine. For large storage rings the empirical scaling law $Q \sim \sqrt{R}$ applies [4], with R in units of meters.

In order to avoid resonant growth of the betatron oscillations, excited by unavoidable misalignments and imperfections, the machine lattice is tuned in such a way that Q is neither an integer nor a simple fraction. More generally, if non-linearities are present in the guide field, the condition

$$nQ_x + mQ_y = p \quad , \quad (1.5)$$

where n, m, p are integers and Q_x and Q_y the horizontal and vertical tunes, is potentially harmful to the stability of betatron motion and is called an *optical resonance* of order $|n| + |m|$.

Figure 1a) shows an example of a typical betatron function in a storage ring with periodicity 12; in Fig. 1b) the corresponding phase advance as defined by (1.3) is plotted. One can see that the phase advances rapidly where the betatron function is low and more slowly in correspondence to higher values of β , but in the average it wiggles about a linear increase.

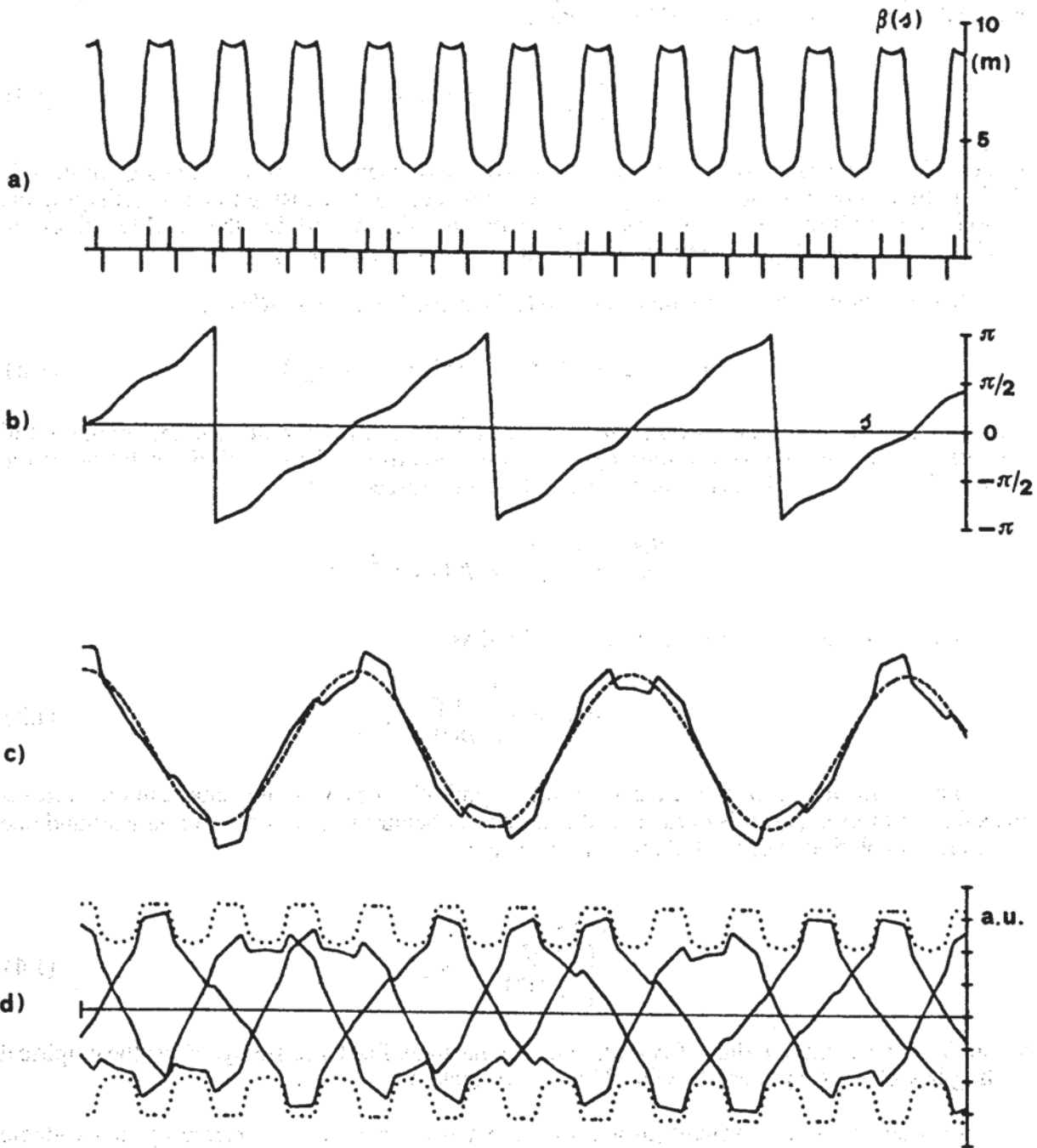


FIG. 1 - a) Example of horizontal betatron function $\beta(s)$ in Adone (periodicity 12). The ticks mark the position of focusing and defocusing quadrupoles. - b) Plot of the betatron phase advance $\mu(s)$ modulo π . - c) Betatron oscillation (solid line) and its smooth approximation (dashed line). - d) Plot of several betatron oscillations with different values of the reference phase ϕ_0 . The dotted line is the envelope of the betatron oscillations around the machine.

Such behavior of the betatron phase advance is quite general and leads to the introduction of the *smooth approximation*, whereby the betatron oscillation is approximated with the sinusoidal trajectory of a particle in a continuous, uniform focusing field; the phase advance is written as

$$\mu_{SA}(s) = \frac{s}{\beta_n} \quad \text{with} \quad \beta_n = \frac{R}{Q} ,$$

and the amplitude of the betatron oscillation is

$$z_{SA}(s) = \sqrt{\varepsilon \beta_n} \cos \left[Q \left(\frac{s}{R} \right) - \phi_0 \right] .$$

A betatron oscillation along with its smooth approximation is shown in Fig. 1c). Introducing the angular frequency of revolution $\omega_0 = v/R$ with v the particle's velocity, t time and $s = vt$, we can also write, as a function of time

$$z_{SA}(t) = \sqrt{\varepsilon \beta_n} \cos (Q \omega_0 t - \phi_0) . \quad (1.6)$$

The *betatron frequency* is the average rate of change of the phase advance and is denoted by $\omega_\beta = Q \omega_0$.

2. BEAM SPECTRA

The material presented in this section is mostly drawn from the treatment made by R. Littauer in [5].

2.1 Longitudinal Spectra

A single particle rotating in the central orbit of an accelerator is described by a time-dependent *linear charge density*

$$\lambda(t) = \frac{e}{v} \sum_{k=-\infty}^{\infty} \delta(t - kT_0) , \quad (2.1)$$

with e the particle's charge, T_0 the revolution time $T_0 = 2\pi R/v$ and $\delta(t)$ the impulse function.

By expressing (2.1) as a Fourier series, we can write

$$\lambda(t) = \frac{e}{v T_0} \sum_{n=-\infty}^{\infty} \exp(jn\omega_0 t) = \frac{e}{2\pi R} \sum_{n=-\infty}^{\infty} \cos(n\omega_0 t) . \quad (2.2)$$

Note that the spectrum contains infinite positive and negative harmonics of the revolution frequency.

If the velocity is close to that of light, as it is the case for relativistic particles, the electric and magnetic field accompanying the particle are confined in a thin pancake perpendicular to the direction of motion, with angular extent $1/\gamma$, where γ is the ratio of particle energy to the rest energy, resembling the TEM field distribution in a coaxial line.

A longitudinal pick-up couples to the particle field and delivers a signal proportional to the linear charge density, whose harmonic content copies that of (2.2) at least up to frequencies of the order $\approx \gamma c/b$, with b the effective radius of the beam pipe and c the speed of light, after which, due to the opening angle of the fields, cut-off occurs. The finite pick-up length also contributes to the attenuation of high frequency components of the longitudinal signal; moreover, if, instead of a single particle, we consider a collection of many particles confined in a length $\approx \sigma$, the signal spectrum starts to drop at angular frequencies of the order $\approx c/\sigma$.

2.2 Transverse Spectra

A suitable configuration of pick-up's yields a beam position monitor (BPM), used to measure the transverse position (see Fig. 2). A BPM is usually sensitive also to the current intensity so that the measured quantity is actually proportional to the the *linear dipole density* d , defined as the product of the linear charge density λ and the position z .

$$d = \lambda * z$$

Let's write the position z as the superposition of two terms

$$z(t) = z_0 + \hat{z} \cos(\omega_\beta t) \quad (2.3)$$

where z_0 is a stable offset due for example to a closed orbit distortion or to a BPM misalignment and the second term is the oscillatory one, due to the betatron oscillation (see Fig. 2).

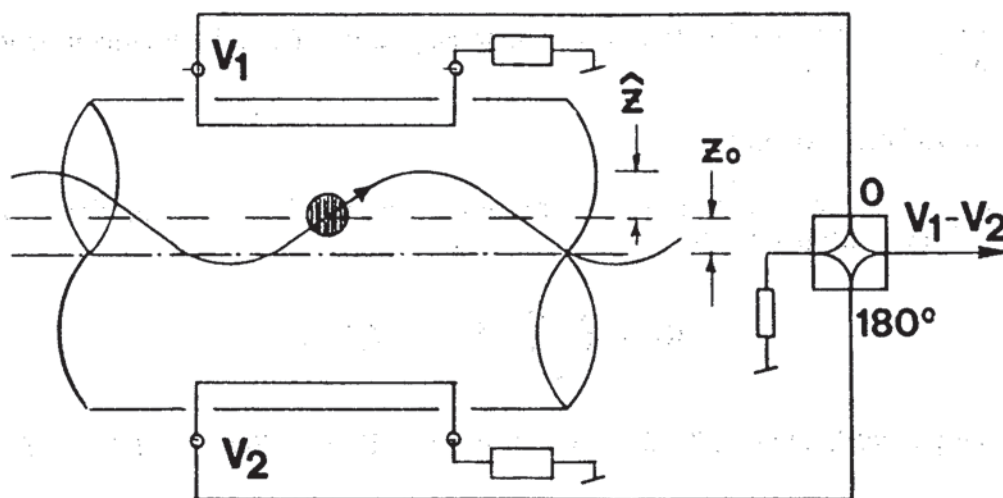


FIG. 2 - Schematic drawing of a Beam Position Monitor. The signals from two strip-line electrodes are wide-band subtracted by means of a hybrid junction to suppress the common-mode signal.

The resulting linear dipole density is then obtained by multiplying (2.2) by (2.3)

$$d = z_0 \frac{e}{2\pi R} \sum_{n=-\infty}^{\infty} \cos(n\omega_0 t) + \hat{z} \frac{e}{2\pi R} \sum_{n=-\infty}^{\infty} \cos(n\omega_0 t) \cos(\omega_\beta t) \quad (2.4)$$

The first term in (2.4) does not contain information about the betatron motion, but only about the closed orbit. Unless the closed orbit is of interest, it is usually rejected by electronic means, or by centering the beam or even by centering the BPM itself [6].

Taking into account only the second term in (2.4), the linear dipole density may be written as

$$d = \hat{z} \frac{e}{2\pi R} \sum_{n=-\infty}^{\infty} \cos[(n+Q)\omega_0 t] \quad , \quad (2.5)$$

showing the appearance of a whole set of side-bands beside the harmonics of the revolution frequency, produced by the non-linear operation of sampling the betatron motion at finite intervals of time.

It is interesting to express (2.5) in terms of positive frequencies only, as seen with a conventional spectrum analyzer (remember that frequency differs from angular frequency by the numerical factor 2π). To this purpose we first write $Q = M + q$, with M the integer part of Q and q the fractional part, and obtain

$$d = \hat{z} \frac{e}{2\pi R} \left\{ \cos(q\omega_0 t) + \sum_{n'=1}^{\infty} \cos[(n' \pm q)\omega_0 t] \right\} \quad , \quad (2.6)$$

where the index $n' = n + M$ has been introduced.

The components of the spectrum (2.6) with $+q$ are called *fast waves*. Those with $-q$ are called *slow waves*. If the value of q is less than 0.5 the fast waves stand at the high-frequency sides of the revolution harmonics and the slow waves at the low-frequency sides; the opposite holds true when q is greater than 0.5.

Examining (2.6), we see that a whole set of ghost frequencies or *aliases* at distance $\pm q\omega_0$ from the revolution harmonics, plus a low-frequency line near DC (base-band) at $q\omega_0$, not present in the original betatron motion, appear in the BPM spectrum. Each of them fits exactly the particle position at the BPM, as shown in Fig. 3. Therefore the measurement of the betatron spectrum with a spectrum analyzer (actually by any instrument, as long as we use a single BPM) only determines the fractional part q of the tune; the information about the integer part of tune is lost.

This ambiguity is a consequence of under-sampling the betatron oscillation, so that we are not able to reconstruct the original signal from the information contained in the sampled data. Indeed, Shannon's sampling theorem [7] states that in order to reconstruct exactly a wave-form, we should sample it at a frequency at least double its highest frequency content. In our case we sample at the revolution frequency a wave-form, the betatron oscillation, whose frequency is Q times larger than the sampling frequency.

If we replace the BPM by a device which kicks the beam transversally at each passage, any frequency appearing in the observed betatron spectrum may be resonantly excited.

2.3 Longitudinal Spectra with Synchrotron Satellites

In the presence of the longitudinal focusing produced by an RF accelerating cavity, a particle beam is bunched and the single particle undergoes synchrotron oscillations of the instantaneous energy.

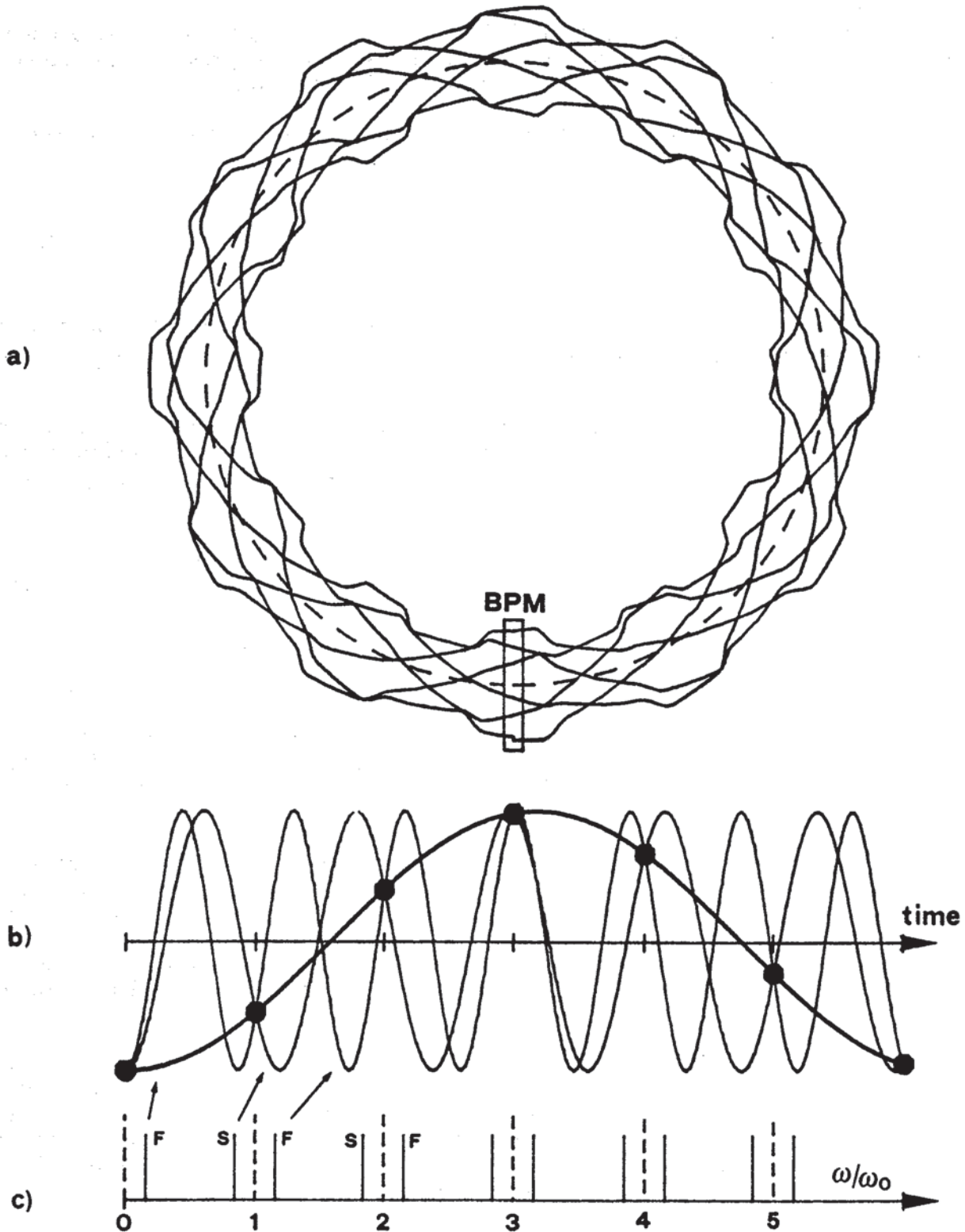


FIG. 3 - a) Betatron motion (exaggerated) of a single particle, traced over 7 successive passages across a BPM. The betatron tune is $Q \approx 3.2$. - b) Heavy dots mark the beam position vs. time at the BPM. The superposed sinusoidal waveforms are the first few betatron modes fitting the beam position. - c) Spectrum analyzer representation of the waveforms. The dashed lines are the harmonics of revolution frequency, the solid lines labeled F are the fast waves and those labeled S are the slow waves.

The angular frequency of revolution is affected according to

$$\frac{d\omega}{\omega_0} = -\eta \frac{dp}{p_0} \quad , \quad (2.7)$$

where $d\omega$ is the frequency variation, dp is the instantaneous momentum deviation with respect to the nominal value p_0 and η is defined by

$$\eta = \left(\frac{1}{\gamma_t^2} - \frac{1}{\gamma^2} \right) \quad , \quad (2.8)$$

where γ_t is the transition energy at which the increase of velocity corresponding to a momentum increase is compensated by the increase of orbit length, thus leaving the revolution time unaltered. The term $(1/\gamma_t)^2$ is also called the *momentum compaction factor* α_c . At ultra-relativistic energies the second term in (2.8) becomes negligible and (2.7) is written

$$\frac{d\omega}{\omega_0} \approx -\alpha_c \frac{dp}{p_0} \quad .$$

The time between successive passages measured at the monitor is now

$$T_0 + \tau = T_0 \left[1 + \frac{\tau_s}{T_0} \cos(\Omega_s t + \psi) \right] \quad , \quad (2.9)$$

where Ω_s is the angular frequency of the synchrotron oscillation, ψ is a phase constant, τ_s is the maximum amplitude of time-modulation and

$$\left(\frac{\tau}{T_0} \right) = - \left(\frac{d\omega}{\omega_0} \right) \approx \frac{d\tau}{dt} \quad . \quad (2.10)$$

In this case the linear charge density is

$$\lambda(t) = \frac{e}{v} \sum_{k=-\infty}^{\infty} \delta(t - kT_0 - \tau) \quad .$$

Using

$$\exp [jx \cos(y)] = \sum_{m=-\infty}^{\infty} (j)^m J_m(x) \exp(jmx)$$

and (2.2), we can express the linear charge density as a Fourier series

$$\lambda(t) = \frac{e}{2\pi R} \sum_{n, m=-\infty}^{\infty} (-j)^m J_m(n\omega_0 \tau_s) \exp [j(n\omega_0 + m\Omega_s) t + m\psi] \quad . \quad (2.11)$$

Each original line in the spectrum (2.2) has now degenerated into an infinite set of satellites right and left at $\pm\Omega_s, \pm 2\Omega_s, \dots, \pm m\Omega_s$ with the amplitudes modulated by the Bessel functions of the first kind of order m, J_m .

The argument $n\omega_0\tau_s$ corresponds to the phase-modulation index used in telecommunications. Although there is a nominally infinite number of sidebands, only a finite number are of appreciable amplitude: namely the coefficients $J_m(n\omega_0\tau_s)$ fall-off very rapidly beyond $m \sim n\omega_0\tau_s$. The first few Bessel functions are sketched in Fig. 4.

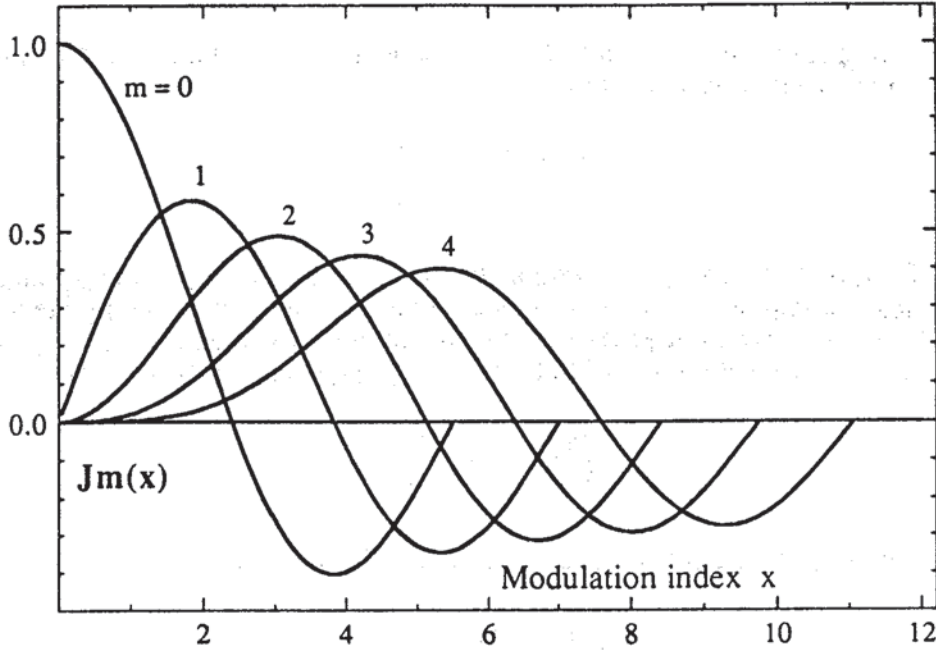


FIG. 4 - Qualitative sketch of the behavior of the Bessel function $J_m(x)$.

2.4 Transverse Spectra with Synchrotron Satellites

If we now include the betatron motion, we must also take into account the modulation of the betatron tune due to the energy modulation. In fact the machine lattice focuses differently particles with energy deviating from the nominal value. The chromaticity of a machine is defined as the relative change in tune of a particle with relative momentum deviation dp

$$\xi = \text{chromaticity} = \frac{dQ}{dp} \cdot \frac{p_0}{Q_0} \quad , \quad (2.12)$$

where Q_0 is the tune value pertaining to the synchronous particle.

According to the above definition, the rate of change of the betatron phase in presence of energy oscillations is then, to first order,

$$\dot{\mu}_\beta = \omega_\beta \approx \omega_0 Q_0 \left(1 + \frac{d\omega}{\omega_0} + \frac{dQ}{Q_0} \right) = \omega_0 Q_0 \left[1 - \frac{\tau}{T_0} \left(1 - \frac{\xi}{\eta} \right) \right] \quad (2.13)$$

and, taking into account the time dependence (2.9) of the time of passage and its rate of change (2.10), the betatron phase is

$$\mu_\beta(t) = \omega_0 Q_0 t + (\omega_\xi - \omega_0 Q_0) \tau_s \cos(\Omega_s t + \psi) \quad , \quad (2.14)$$

where the chromatic frequency $\omega_\xi = (\xi Q_0 / \eta) \omega_0$ has been introduced.

The expression of the linear dipole density d is now written, taking into account (2.11) and (2.14), as

$$d(t) = \frac{e \hat{z}}{2\pi R} \sum_{n, m=-\infty}^{\infty} (-j)^m J_m \{ [(n+Q)\omega_0 - \omega_\xi] \tau_s \} \exp[j(\omega_{nm} t + m\psi)], \quad (2.15)$$

with the *mode frequency* $\omega_{nm} = (n+Q)\omega_0 + m\Omega_s$.

Here we have again infinite synchrotron satellites around the betatron lines, but, due to the tune modulation (2.13), the amplitude envelope function is shifted by the chromatic frequency ω_ξ . Thus, examining with a spectrum analyzer (positive frequencies only) the slow and fast waves near a harmonic of the revolution frequency, the amplitude of synchro-betatron modes above and below may be quite different due to the different argument of the Bessel function coefficient. Namely, around the sides of the n -th revolution harmonic the amplitude is modulated by

$$\begin{aligned} \text{Fast waves} &\rightarrow \left| J_m \{ [(n+q)\omega_0 - \omega_\xi] \tau_s \} \right| \\ \text{Slow waves} &\rightarrow \left| J_m \{ [(n-q)\omega_0 + \omega_\xi] \tau_s \} \right| . \end{aligned}$$

2.5 Spectra of many Particles

So far we have considered the somewhat idealized case of a single particle. If we turn to the realistic situation of a collection of many particles, several effects have to be considered.

First of all, we must take into account the modification to the static transverse focusing caused by the collective forces of a large number of charged particles within a vacuum chamber, which introduce a driving term in equation (1.1), called the space-charge forcing term. This term and the wake-field term, arising from the image fields on the vacuum chamber acting back on the beam, affect both the center-of-mass motion and the motion of individual particles within the beam, leading to coherent and incoherent tune-shift. The subject is thoroughly discussed in Ref. [8]. In addition, when beams are brought to collision, beam-beam forces also cause incoherent tune-shift.

Secondly, associated with a distribution of momentum spread, there is a spread of revolution frequencies and tunes, according to (2.7) and (2.13), and the spectra (2.2), (2.5), (2.11) and (2.15) are effectively averaged over the entire distribution. In Fig. 5, we show an example of a measured betatron spectrum exhibiting synchrotron satellites.

A BPM is sensitive to coherent motion and an external kicker excites coherent oscillations, so that the stimulus-response approach to measure the betatron tune, only applies to the coherent tune. Other indirect methods have been devised to study the incoherent tune-shift and incoherent tune distribution [8-10].

In a coasting beam the particles are randomly distributed around the machine and the time average of spectra (2.2) over all the particles is null, except for the DC component (the average current). On the other hand, if we take the rms average of the spectrum over a finite bandwidth in frequency domain around a revolution harmonic, a signal of finite power results from the statistical fluctuations of the large, though finite, number of particles [11-13]. This is called the *Schottky noise signal* and its average power per observation bandwidth is proportional to the number of particles N .

DATA 09/06 ORE 12.02
 FASCIO DI POSITRONI (3 BUNCHES) Ibeam = 0.92 mA
 ENERGIA = 1500 MeV ; tau damping = 11 n sec
 CORRENTE NEI Q-POLI "F" : 300 Amp.
 CORRENTE NEI Q-POLI "D" : 376 Amp.
 TENSIONE DI RADIO-FREQUENZA : 130 KV
 AMPIEZZA TENSIONE DI ECCITAZIONE : 6.2 V Twait = 33 msec
 SWEEP UP
 Qx = 3.0645
 MASSIMO ALLARGAMENTO : 9 %
 SIDEBANDS DI SINCROTRONE A 3.73 KHz

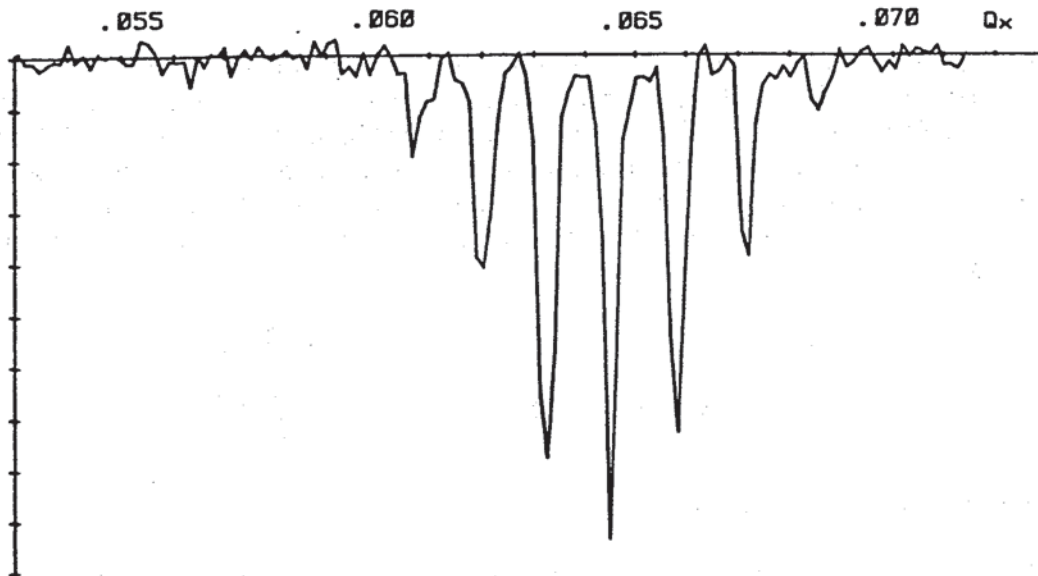


FIG. 5 - Example of a base-band betatron spectrum exhibiting synchrotron satellites, measured in ADONE. The negative appearance is non-essential.

The Schottky noise has been first observed in ISR and has been put to good use for non-destructive beam diagnostics in proton machines and to very welcome use for stochastic cooling of longitudinal and transverse emittance of antiproton beams.

The same principle is used to monitor the incoherent betatron motion, although the signal level is much lower in this case and clever low-noise design in the detector electronics is mandatory.

In the case of bunched beams, the transverse Schottky signal is also present, but the common-mode - the first term in (2.4) - signal power, proportional to N^2 , tends to obscure it. Then, selective filtering and careful beam centering is required. A transverse detector for bunched proton beams, implemented at CERN-SPS, is described in Ref. [6].

3. BEAM POSITION MONITORS AND KICKERS

In this Section we briefly review various types of *Beam Position Monitors* (BPM) and kickers and notice some differences which play a rôle in the measurement of tune.

3.1 Beam Position Monitors

The literature about BPM's is abundant; we cite as general reference the excellent reviews by Littauer [5], Borer-Jung [14] and Pellegrin [15].

Beam pick-up's are discontinuities in the vacuum chamber of an accelerator, which interrupt and divert into a measuring device part of the wall image-current of the beam. They are sensitive to the electric field of the beam, to the magnetic field, or both and deliver to the outside world a voltage or current signal proportional to the instantaneous beam charge. The pick-up transfer characteristics include the effects of the beam distance from it.

A suitable combination of pick-up signals yields a beam position information. The operation can be made directly at the BPM, e.g. by subtracting the signals from two opposing pick-up's by means of wide-band hybrid junctions, or by digitizing the single p.u. signals and computing later the beam position by extrapolation of a calibration table. The latter method is obviously slower and its application in detecting betatron oscillations is possible only when the time interval between successive beam passages is large (e.g. : LEP $\sim 89 \mu\text{s}$) and adequate computing power is available; otherwise it is generally employed to measure the DC closed orbit distortion.

Among BPM's sensitive to the electric field of the beam we mention the *split electrodes* or *plates* and the *buttons* (see Fig. 6). The large dimensions of the former make them highly sensitive and the linear diagonal cut renders the difference signal linearly dependent on the beam position.

The button monitors (usually four buttons are employed to yield horizontal and vertical position) are generally less sensitive to the beam current and inherently non-linear with respect to the beam position, but a large number of them is allowed in a storage ring, owing to their small parasitic longitudinal and transverse coupling impedance. They are mainly utilized for orbit measurement.

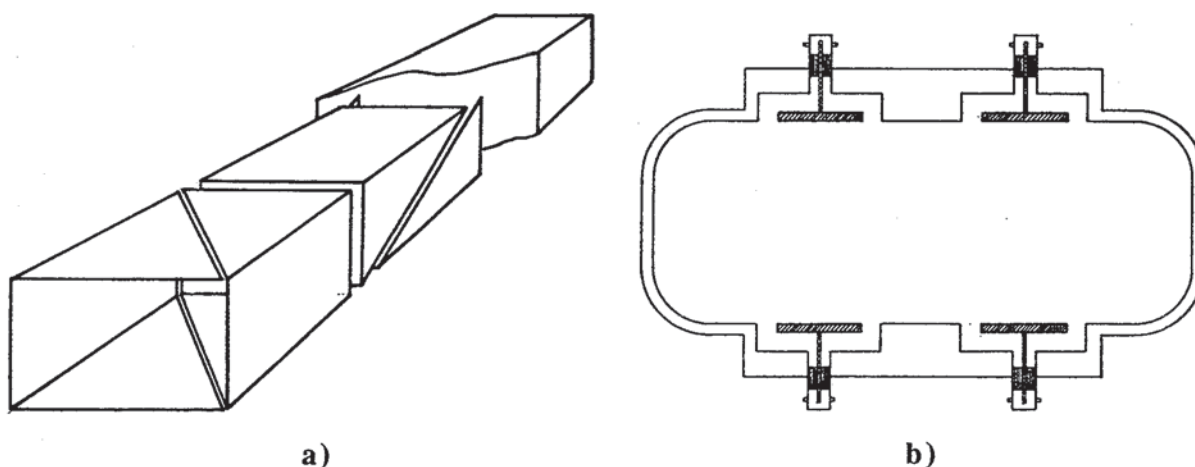


FIG. 6 - Electrostatic Beam Position Monitors: a) Split electrodes, b) Buttons.

Small loops in the vacuum chamber (see Fig. 7) couple to the beam magnetic field. A variation of the loop is a short strip-line short-circuited to the vacuum chamber at one end [16].

The usual equivalent circuit representation of an electrostatic monitor is a current generator of the same value of the portion of the image current intercepted by the monitor, shunted by the electrode capacitance to ground.

The equivalent circuit of a magnetic loop is a voltage generator with a series inductor. The voltage is proportional to the rate of variation of magnetic flux associated with the beam current and linked to the loop, the series inductance is the self-inductance of the loop.

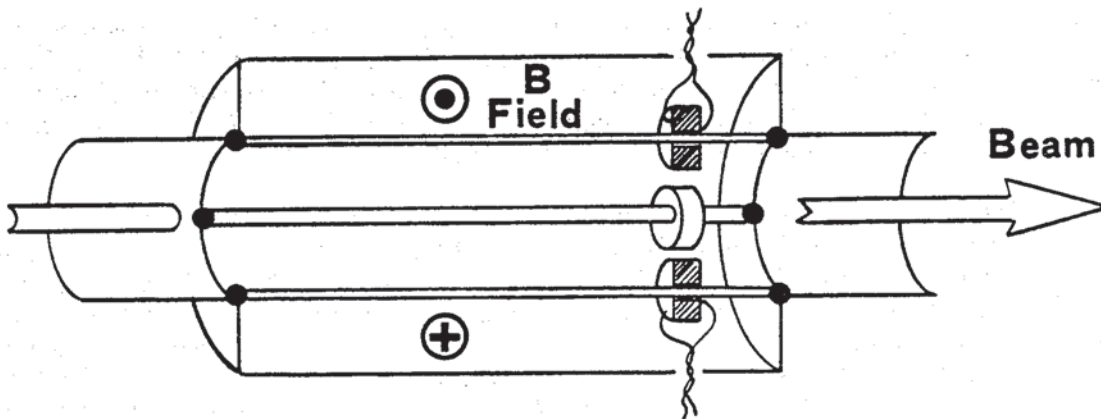


FIG. 7 - Monitor coupling to the magnetic field of the beam. From Ref. [14].

The sensitivity of electrostatic and magnetic monitors to both beam current and position may be widely different, depending mostly on the size, shape, bandwidth of observation, size of the surrounding vacuum chamber and read-out circuitry, rather than on the type of monitor. Thus there is no point in comparing the virtues of one class of monitors with respect to the other.

It is worth noting, however, the following important difference between electrostatic and magnetic monitors [5, 17]: if an electrostatic BPM is employed to observe the betatron motion of colliding beams of opposite polarities at the *Interaction Point* (IP), most of the electric fields of the two beams cancel each other, except for the contribution of the out-of-phase betatron motion, the so-called π -mode. At the IP, only the π -mode is measurable with electrostatic monitors.

On the other hand, if a magnetic monitor is used, the contributions to the magnetic field by the opposite beams oscillating in-phase, the σ -mode, add-up, while those relative to the π -mode cancel. Thus we can selectively observe one or the other of the normal modes of beam-beam oscillations depending on the type of monitor used.

If the BPM is at a location away from the IP and the betatron motion is observed at a mode frequency ω_m , the relative phase difference between the betatron motion of the opposing beams is

$$\Delta\phi = 2(\mu - \omega_m T) \quad ,$$

with T the time-of-flight between the IP and the monitor position and μ the betatron phase advance. Now if $\Delta\phi$ is a multiple of 2π , the same considerations as above apply and the selectivity of the monitor is the same as that at the IP; if $\Delta\phi$ is an odd multiple of π , the mode selectivity is opposite to that at the IP.

The *strip-line* is an electrode usually longer than the characteristic bunch length, which forms with the vacuum pipe a transmission line of characteristic impedance Z_0 . By a suitable choice of the ratio between the strip width and distance from the pipe, the characteristic impedance is made 50Ω . The electrode is terminated at both ends via a coaxial vacuum feed-through into resistive loads matched to Z_0 (see Fig. 8).

In a strip-line monitor both the electric and the magnetic field contribute to the output signal but the beam electromagnetic field and the wave field in the transmission line interfere constructively at one port and destructively at the other yielding directional properties [5, 14, 15, 18].

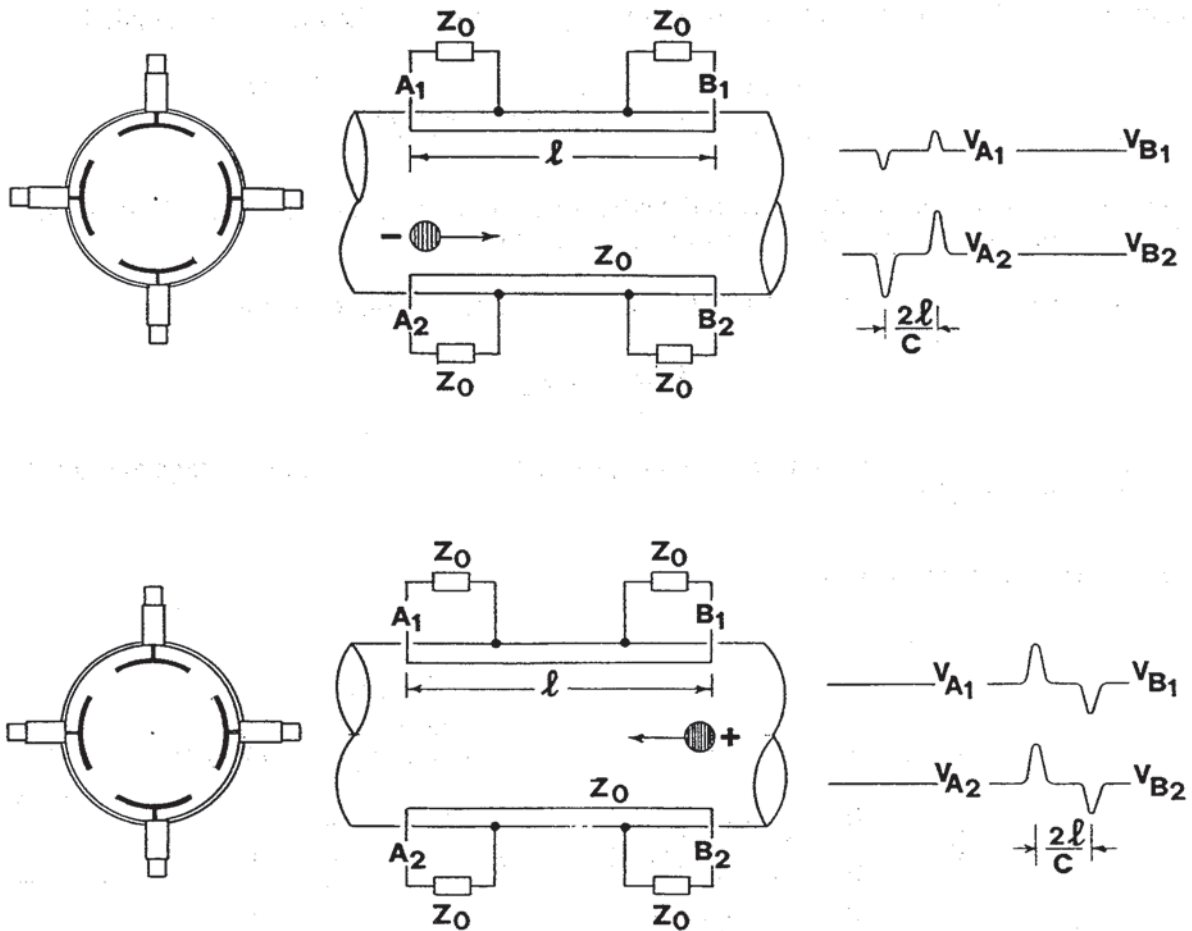


FIG. 8 - Schematic representation of a directional strip-line monitor with beams of opposite velocity and charge, along with a qualitative sketch of the voltages at the output ports.

In principle we get a useful signal only at the up-stream port of the monitor. The voltage at the up-stream load resistor appears as a doublet of pulses of opposing polarity reproducing the longitudinal time distribution of the beam current and separated in time by an interval $\Delta t = 2l/c$, where l is the length of the strip. No signal appears at the down-stream port as long as the beam velocity and the propagation velocity in the strip are equal (for ultra-relativistic beams this means a minimum or null amount of dielectric in the vicinity of the strip) and the load resistor is exactly matched. In practice any mismatch introduced, for example, by the vacuum feed-throughs or mechanical imperfections, tends to spoil the directional properties of the monitor.

The directionality of the strip-line monitor is particularly useful with colliding beams, if one wants to measure only one beam position in presence of the other beam.

The time-domain voltage response of the matched strip-line is, at the up-stream port and for a centered beam [14, 15, 18]

$$v(t) \approx \frac{Z_0}{2} \left(\frac{\alpha}{2\pi} \right) \left[i_b(t) - i_b\left(t - \frac{2l}{c}\right) \right],$$

with α the opening angle of the strip, $(\alpha/2\pi)$ the factor of coverage and $i_b(t)$ the instantaneous beam current. The corresponding complex coupling impedance in the frequency domain is

$$Z_c(j\omega) \equiv \frac{V(j\omega)}{I_b(j\omega)} \approx Z_0 \left(\frac{\alpha}{2\pi} \right) \sin \left(\frac{\omega l}{c} \right) e^{j \left(\frac{\pi}{2} - \frac{\omega l}{c} \right)},$$

where $V(j\omega)$ and $I_b(j\omega)$ are the spectral densities of the output voltage and of the beam current. The response is maximum at frequency $f = c/4l$, or odd multiples.

The position sensitivity to a small beam displacement Δz from the center line is

$$\frac{b}{2} \frac{\Delta V}{\Sigma V} \approx \Delta z,$$

where ΔV is the difference voltage of two opposing strips, ΣV is the sum voltage and b is the vacuum chamber radius.

3.2 Beam Size Monitors

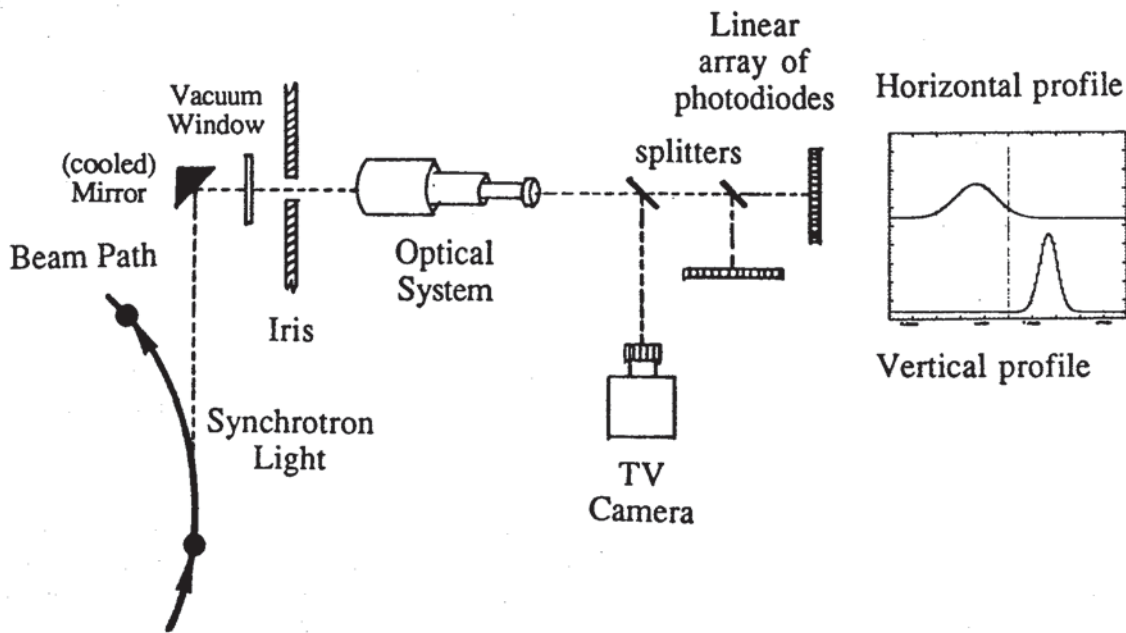


FIG. 9 - Schematic view of a synchrotron light monitor station.

Beam size monitors are mentioned here because they can give useful information about the incoherent betatron motion. For example, as we shall see later, the coherent and incoherent beam response to an external transverse kick may be quite different and we are interested in investigating both.

A BPM may be turned into a beam dimension monitor by exploiting the non-linear response with respect to the position. In other words it is possible to connect the various electrodes forming a BPM in such a way as to make the response sensitive to the beam aspect ratio [19].

The favourite beam dimension monitor, at least at electron facilities, is, however, the *synchrotron radiation monitor*. Due to the high directionality of the synchrotron radiation, the spatial distribution of the emitted light reproduces fairly well the transverse distribution of charge density in the beam. By projecting the light onto some slit or pinhole, an accurate measurement of the charge density can be obtained by means of a photodetector [20]; moreover the beam size may be easily observed and measured at a TV monitor (see Fig.9). Although such a monitor comes naturally only with electrons, its use at high-energy proton machines is also reported [21].

3.3 Transverse Kickers

Transverse *kickers*, or *shakers*, are used to excite transverse modes by the application of a rapidly varying external field.

As in BPM's, the deflecting field can be electric, magnetic or a combination of the two. For example, in open plates driven by a voltage generator, there is an electric field normal to the plates, while in the region inside shorted coils driven by a current generator, a magnetic field is present (see Fig. 10).

The capacitor formed by the plates and the inductor formed by the coils may be made part of an L-C resonant circuit to reduce the power requirement of the driving amplifier.

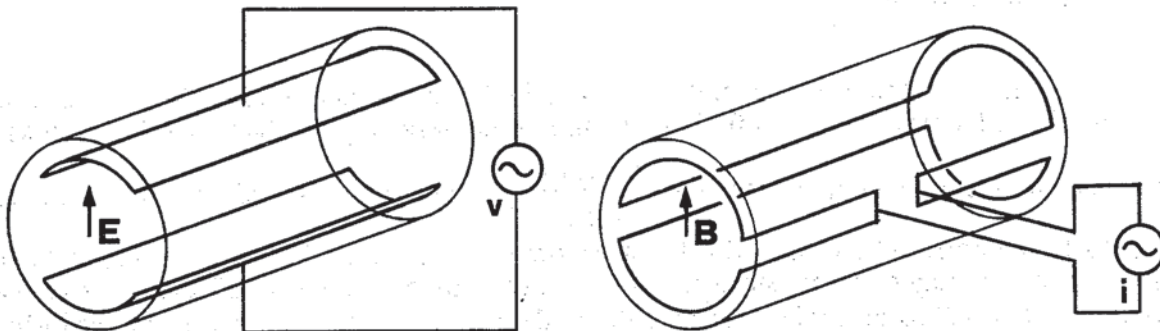


FIG. 10 - *Electric kicker in the form of open plates (left) and magnetic kicker formed by shorted coils (right).*

The same considerations as in the case of BPM's apply to electric and magnetic kickers for the selective excitation of the normal modes of colliding beams.

The matched strip-line, when used as a transverse kicker, maintains the directional properties described in section 3-1. Power is applied at the down-stream port and the combination of magnetic field due to the current flow along the strip, and electric field due to the strip being at non-zero potential, gives a net deflecting Lorentz force.

The electric and magnetic forces add-up if the external voltage is applied at the down-stream port, while they cancel when the power flow is in the same direction as the beam velocity (see Fig. 11). Then, in the case of colliding beams, it is possible to excite selectively one beam without effect on the other.

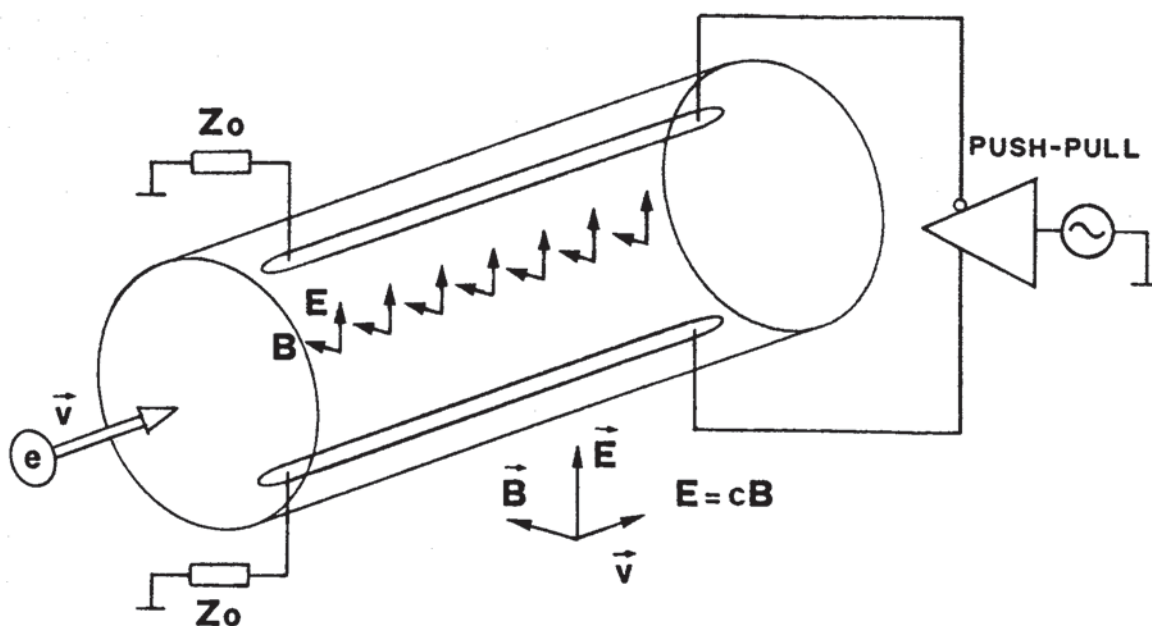


FIG. 11 - Strip line kicker. If the beam and the voltage wave enter the strip-line from opposite directions, the magnetic and electric force add-up and give a deflection. If the voltage wave and the beam velocity are in the same direction the two forces cancel and there is not net deflection.

In contrast with the former two, the strip-line kicker presents a constant load-impedance to the amplifier feeding it. The useful bandwidth is relatively large: in fact the efficiency as a function of frequency is proportional to $\propto \frac{\sin(\omega l / c)}{(\omega l / c)}$ and retains the directional properties down to frequencies where the skin depth becomes larger than the width of the vacuum chamber and the magnetic field starts leaking out of the pipe. The kicker efficiency is zero at frequencies $f = c/2l$ or multiples, because the deflecting force encountered in the strip-line region is in one direction for half a transit time and in the opposite direction for the other half.

4. TUNE MEASUREMENTS

As in circuit theory, the beam response may be analyzed in terms of stimulus-response correlation either in the time domain or in the frequency domain. The two methods are mathematically equivalent: the pulse and frequency response are related to each other by a Fourier transform pair.

4.1 Time Domain

Measuring the beam response to a transverse excitation of short duration corresponds to studying the transient response of a circuit to a delta pulse.

The stimulus is provided by a fast transverse force produced by a kicker magnet and lasting for a time less than a revolution period, which excites coherent betatron oscillations. An injection kicker is sometimes used. The response is the beam transverse position detected by a beam position monitor.

The fractional part of the tune can be determined in the simplest way by displaying the BPM signal at an oscilloscope, measuring the frequency of the pseudo-oscillation which modulates the position signal and dividing by the revolution frequency.

Another method consists in amplitude-detecting and limiting the BPM signal and, with a frequency-meter, gated in synchronism with the application of the kick, measuring the frequency ratio of the BPM signal to a clock at the revolution frequency; in this way the fractional value of the tune can be directly displayed.

It is also possible to sample and digitize with a fast ADC the beam position at one monitor location, and perform a numerical Fourier analysis on the sampled data to obtain the fractional tune and the tune distribution [22].

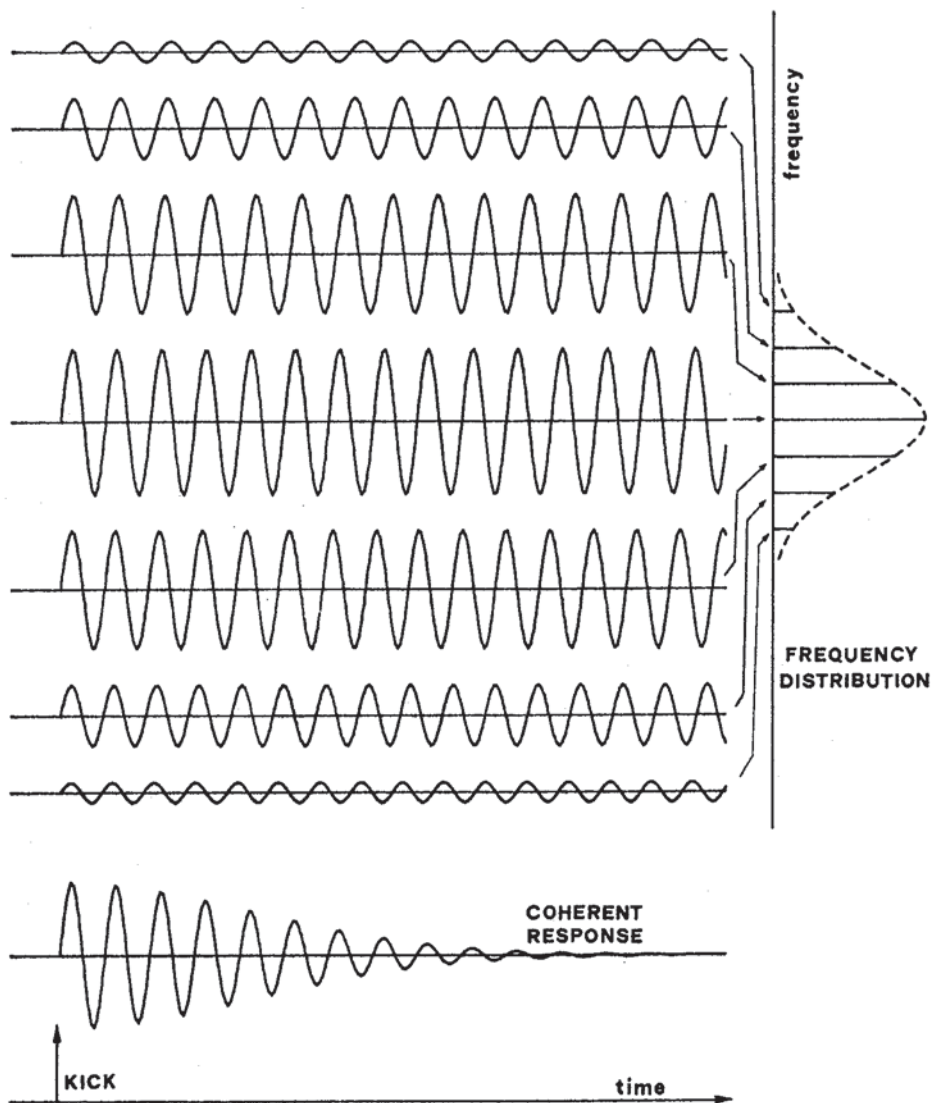


FIG. 12 - Linear superposition of individual betatron oscillations after the application of a transverse kick. The curve at the right side is the distribution of incoherent tunes. In this example we assume a Gaussian distribution around a central value. The curve near the bottom is a plot of the time evolution of the center-of-mass response, as detected by a BPM, showing Landau damping.

Figure 12 shows an example of ensemble response of a collection of particles with a finite tune spread to an external kick. The betatron frequency spectrum in the example is assumed to have a gaussian distribution around a central value. One may think of an electron beam with a finite energy spread due to the emission of synchrotron radiation, which accounts for tune spread via the chromaticity of the lattice.

At the kick instant, each particle starts a free betatron oscillation with the same initial phase but with a frequency slightly different from that of the others. Even if the individual oscillations last for a long time, the resultant coherent response detected by a BPM is damped, as shown, as a consequence of the decoherence of the individual oscillations, in a time interval of the order of the inverse of the spread of the angular frequencies. The time envelope of the coherent response is the inverse Fourier transform of the tune distribution, $F(\omega)$ [23].

The beam size (as measured, for example, with a synchrotron radiation monitor), however, is affected by the amplitude of the individual oscillations and takes much longer to recover, if ever, to the initial value. Electrons are eventually damped because of radiation, but protons are not, so the kick method must be used cautiously with protons because too large a kick may irreversibly deteriorate the transverse emittance to an unacceptable value and lead to beam loss.

The damping of coherent oscillations caused by a spread of the natural frequencies is called *Landau damping*. It is not the purpose of this presentation to go into the details of the several mechanisms which may induce a spread of the tune values. We just list a few of them:

- current ripple in the magnet power supplies;
- incoherent tune-shift depending on momentum, induced by sextupoles;
- incoherent tune-shift depending on amplitude, induced by octupole fields;
- incoherent tune shift due to space charge forces, beam-beam forces and non-linear forces by ions trapped in the beam;
- incoherent momentum spread and non-zero chromaticity.

It is noteworthy that, when measuring the tune with the kick method, the observation time and, therefore, the accuracy of the measurement are limited by the damping.

4.2 Frequency Domain

In the *RF method*, sometimes called the *RF-knockout (RF-KO) method* [8], the stimulus to the beam is a CW transverse force provided by a kicker driven by a swept-frequency sinusoidal generator and the response is the amplitude of the resulting betatron oscillation.

A typical measurement system is basically composed of a swept spectrum analyzer with a tracking generator. The tracking generator is a sinusoidal source whose output frequency exactly follows that instantaneously displayed at the spectrum analyzer. The tracking generator output is used to drive the kicker and the position signal from a BPM is fed to the spectrum analyzer to measure the steady-state amplitude of the beam response. The kicker and the detector can be part of a transverse feedback system, where available.

Due to the longer observation time, the accuracy in resolving frequency is better than with the kick method, on the other hand the direct perception of damping is lost. The tradeoff between the frequency accuracy Δf and the observation time Δt is imposed by the indetermination relation $\Delta f \geq 1 / \Delta t$ [7].

An instrument which provides an RF output and measures the gain ratio and the relative phase between excitation and response altogether is the *network analyzer*. With such an instrument the *Beam Transfer Function (BTF)* can be measured. In Fig. 13 a schematic layout of a BTF measurement is shown. In Fig. 14 we show an example of a tune measurement made with the above instrumentation.

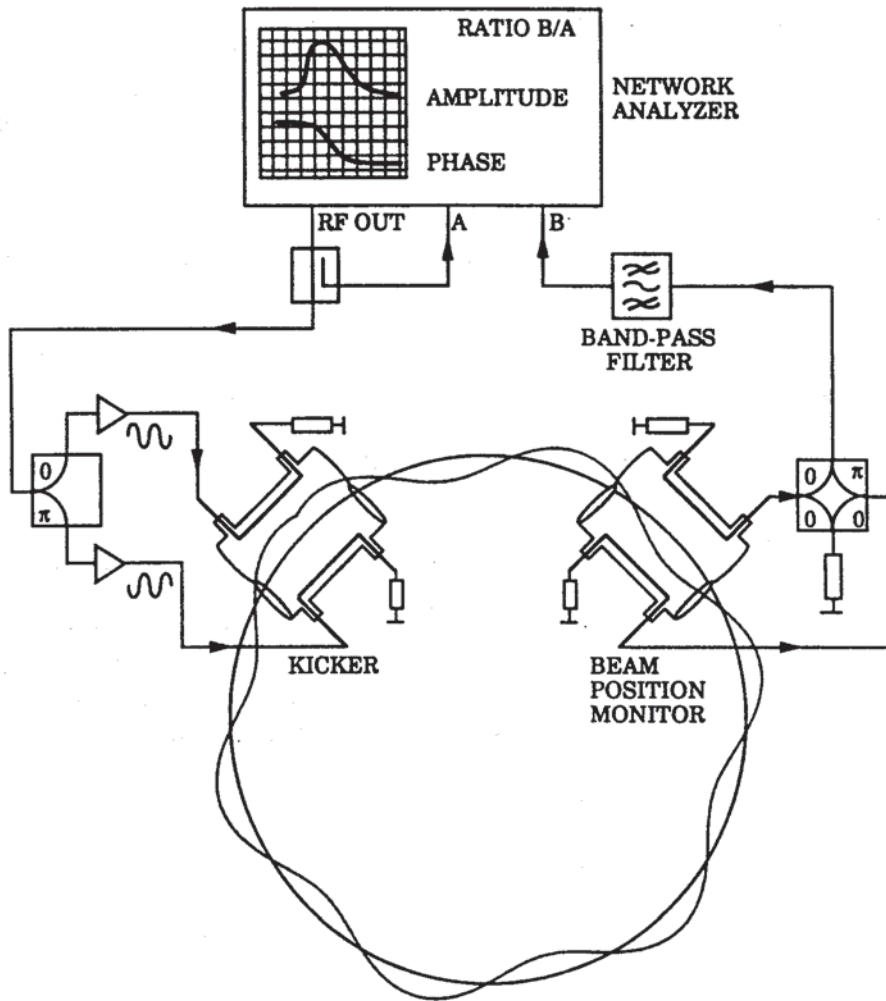


FIG. 13 - Schematic layout of a Beam Transfer Function measurement system.

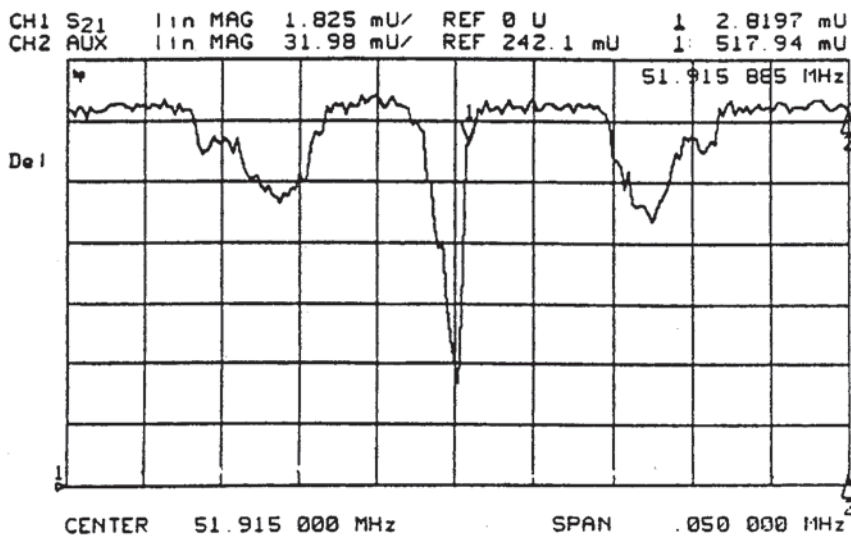


FIG. 14 - Example of a measurement of betatron tune distribution with a network analyzer. A sharp betatron line at the center, and two synchrotron satellites are clearly visible.

The Beam Transfer Function is defined as the complex ratio of the transverse velocity response dz/dt to the acceleration $G(t)$ at the kicker, averaged over the tune distribution $F(\omega)$ [12, 13, 23, 24]. The real part of the BTF gives the particle distribution in incoherent tune, while the imaginary part contains information about the additional acceleration from the transverse forces generated by the interaction of the beam with the parasitic impedance of the machine and fed-back to the beam.

The inverse of the BTF corresponds to the *stability diagram* in the complex plane and gives, as in circuit theory, information about the stability margin, the transverse parasitic impedance and the effective impedance of feedback systems.

In the measurement with a conventional swept spectrum or network analyzer, a long observation time is involved, due to the indetermination relation mentioned above and to the fact that a single frequency line is analyzed at a time. In addition to the intrinsic indetermination, every time we change the frequency we must allow the transient beam response to die-out and the steady-state response to be attained [20].

This problem can be overcome by the use of a *dynamic signal analyzer*, or *digital spectrum analyzer*, which is based on high-speed digital Fourier analysis (Fast Fourier Transform-FFT) executed by an embedded processor. N voltage samples over a period T are digitized and transformed into $N/2$ complex Fourier coefficients, spanning a frequency range from DC to $N/2T$. The frequency resolution is $\Delta f = 1/T$, and the whole spectrum is instantly available, thus the total time of analysis is reduced by a factor $2/N$ with respect to a conventional swept analyzer with the same frequency resolution. The number of frequency points computed is typically ~ 200 to ~ 1000 and the frequency range extends to ~ 100 kHz. Such analyzers usually provide two channels, a pseudo-random noise generator and capability for complex transfer function calculations.

The noise output, applied to a kicker, excites all betatron modes within the band at the same time. A modest power is then enough to produce measurable oscillations without blowing-up the beam. The beam response is cross-correlated with the noise excitation and the complex transfer function is measured [12, 14].

The relatively low operating frequency is no problem, as long as the band of interest is within the maximum frequency of the FFT analyzer. The noise output is up-converted to the frequency of the betatron mode under study and the betatron signal is down-converted to the operating frequency of the analyzer [12]. A schematic layout of a BTF measurement system with a dynamic signal analyzer is shown in Fig. 15.

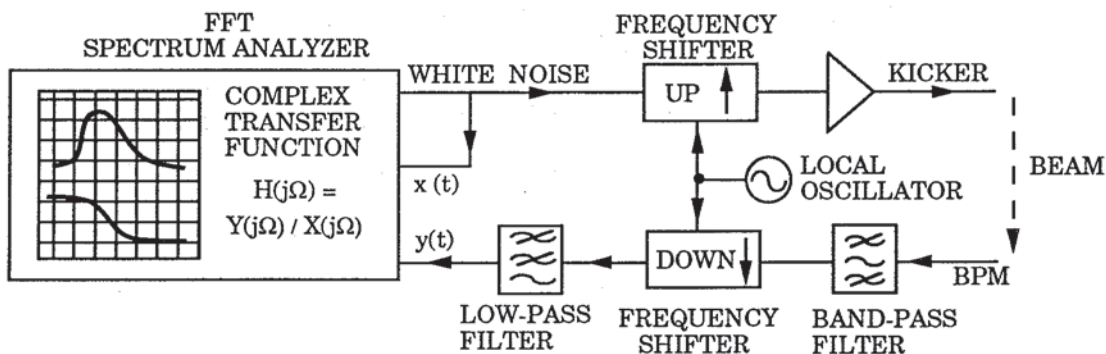


FIG. 15 - Schematic layout of a BTF measurement system with an FFT analyzer.

4.3 Other Methods

A *Phase Locked Loop (PLL)* is a voltage-controlled-oscillator (VCO) which serves itself to the strongest signal frequency of the input signal. A PLL is functionally equivalent to a narrow-band adaptive filter and is commonly used in telecommunications to "lock-on" to very weak frequency-modulated signals and track their central frequency. A PLL can be used for measuring the tune in the configuration of Fig. 16. Small-amplitude betatron oscillations are excited at the VCO frequency; when a lock condition is detected, the output frequency is at the central betatron frequency.

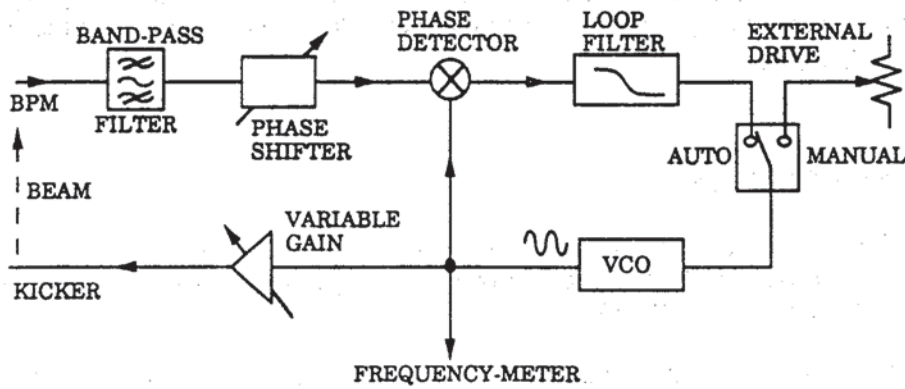


FIG. 16 - Tune measurement with a Phase Locked Loop.

In order to reduce the chance that the PLL locks onto an unwanted mode frequency, it is advantageous to restrict the tracking range in a region close to the chromatic frequency ω_{ξ} (see Section 2), where the synchrotron satellites are weak and the central betatron line is sharp and peaked. If there are residual betatron oscillations, the PLL output can lock onto the central frequency without the need to excite the beam.

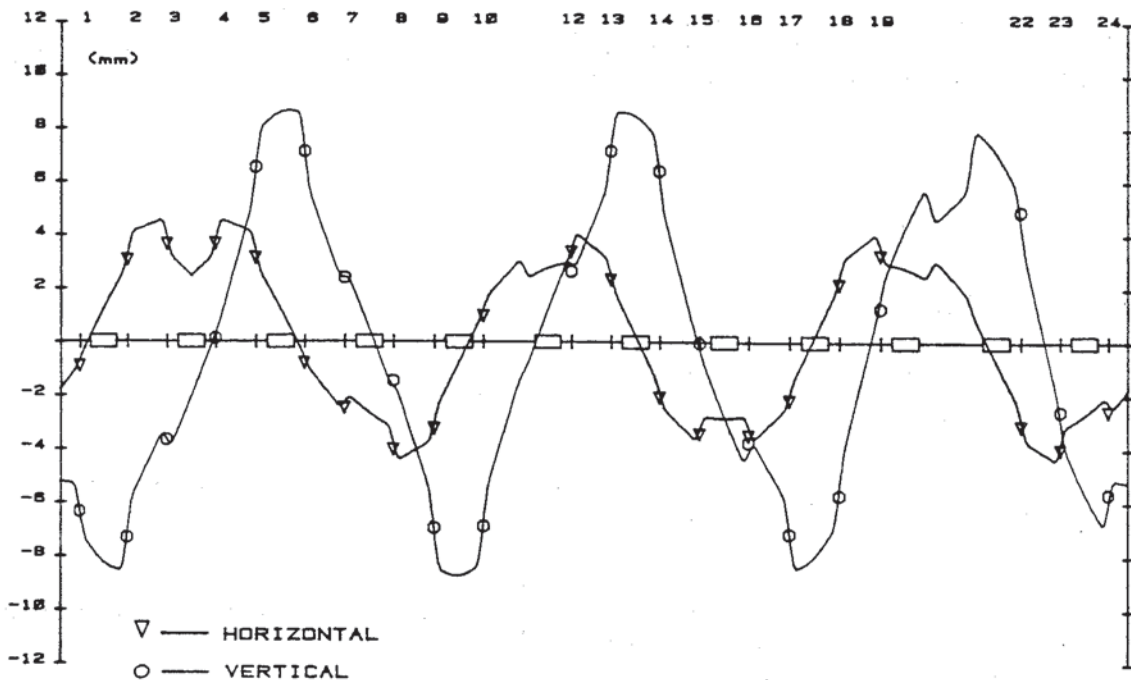


FIG. 17 - Difference orbit with magnetic correctors.

The integer part of Q can be obtained by powering a magnetic corrector and measuring the difference orbit (see Fig. 17). The number of full periods of the resultant closed orbit is the integer part of Q . Moreover, an estimate of the overall Q value can also be obtained by the difference orbit [25]. The number of position monitors must be $> 2Q$ in order to exclude under-sampling. The tune-shift depending on beam current intensity can also be obtained by closed orbit measurements, without perturbing the beam [8, 26].

There is not an *a priori* criterion to determine whether the fractional tune q is above or below 0.5, i.e. if a particular mode observed is a fast or a slow wave (see Sec. 2). However, it can be decided by the following procedure. Suppose we measure the frequency f_β of a betatron mode just above the n -th harmonic of the revolution frequency f_0 . The focusing strength on the plane of interest is then increased and the mode frequency measured again: if the frequency is higher, the observed mode is a fast wave and the fractional tune is $q = (f_\beta / f_0) - n$. If the re-measured mode frequency is lower, the observed mode is a slow wave and the fractional tune is $q = n + 1 - (f_\beta / f_0)$.

5. CONCLUSIONS

The betatron tune measurement, besides involving much interesting Accelerator Physics, is a major diagnostic tool for the optimization of injection, extraction, current intensity and overall performance of accelerators.

In the commissioning phase of a new accelerator, betatron tune measurements are performed to check and correct the real lattice to a precision higher than that obtainable from simulation programs. Tunes are also measured in order to:

- Measure and correct the lattice chromaticity.
- Measure local values of the betatron function and of the betatron phase advance [23].
- Calibrate magnetic elements and create a reliable operational model.
- Fine-tune special insertions.

In routine operation and during machine studies, the techniques exposed in the preceding section are used mainly to:

- Identify dangerous resonances, control coupling, and implement closed loop control.
- Study transverse dynamics and instabilities, study machine impedances, collective phenomena, damping and effectiveness of feedback systems [23-24].

* * *

REFERENCES

- [1] M. Sands, "The Physics of Electron Storage Rings - An Introduction", SLAC Report SLAC-121 (1970).
- [2] E. Keil, "Theoretical Aspects of the Behaviour of Beams in Accelerators and Storage Rings", Editor: M. H. Blewett - CERN 77-13, pp.11-36 (1977).
- [3] K. Steffen, "Basic Course on Accelerator Optics"; E. Wilson, "Transverse Beam Dynamics". CERN Accelerator School - General Accelerator Physics, Proceedings, Editors: P. Bryant, S. Turner. CERN 85-19 (1985).

- [4] A.W. Chao, "Elementary Design and Scaling Considerations of Storage Ring Colliders", in "Physics of Particle Accelerators". Editors: M. Month, M.Dienes - AIP Conference Proceedings No. 153, pp. 103-120 (1987).
- [5] R. Littauer, "Beam Instrumentation", in "Physics of High Energy Particle Accelerators". Editor: M. Month - AIP Conference Proceedings No. 105, pp. 869-953 (1983).
- [6] T. Linnecar, W. Scandale, "A Transverse Schottky Noise Detector for Bunched Proton Beams", IEEE Trans. on Nuclear Science, Vol. NS-28, n.3, p. 2147 (1981).
- [7] A. Papoulis, "The Fourier Integral and its Applications", Mc Graw-Hill Book Company, inc. (1962).
- [8] P. Bryant, "Betatron Frequency Shift Due to Self and Image Fields", CERN Accelerator School - Second General Accelerator Physics Course. Proceedings. Editor: S. Turner - CERN 87-10, p.62 (1987).
- [9] D.Kemp et al., "On-line Q Measurement During Phase-Displacement Acceleration in the CERN ISR", IEEE Trans. on Nuclear Science, Vol. NS-26, n.3, p. 3352 (1979).
- [10] E. Keil, "Intersecting Storage Rings", CERN 72-14, p.28 (1972).
- [11] J. Borer et al., "Non-destructive Diagnostics of Coasting Beams with Schottky Noise", Proceedings of the IX-th International Conference on High Energy Accelerators, SLAC - Stanford, May 1974, p.53 (1974).
- [12] J. Borer et al., "ISR Beam Monitoring System Using Schottky Noise and Beam Transfer Function", CERN-ISR-RF/80-30 (1980).
- [13] D. Boussard, "Schottky Noise and Beam Transfer Function Diagnostics", CERN Accelerator School - Advanced Accelerator Physics, Proceedings, Editor: S. Turner - CERN 87-03, p.416 (1987).
- [14] J. Borer, R. Jung, "Diagnostics", CERN Accelerator School - Antiprotons for Colliding Beam Facilities. Proceedings. Editors: P. Bryant, S. Newman - CERN 84-15, p.385 (1984).
- [15] J.L. Pellegrin, "Review of Accelerator Instrumentation", Proceedings of the XIth International Conference on High Energy Accelerators, CERN, Geneva, July 1980, (Birkhäuser, Basle, 1980),p.459, also SLAC Note SLAC-PUB-2522 (1980).
- [16] J. C. Denard et al., "Parasitic Mode Losses versus Signal Sensitivity in Beam Position Monitors", SLAC Note SLAC-PUB-3654 (1985).
- [17] R. Littauer, M. Placidi: "Beam-Beam Modes in Q-Monitoring", CERN-LEP-555 (1986).
- [18] R. E. Shafer, "Characteristics of Directional Coupler Beam Position Monitors", IEEE Trans. on Nuclear Science, Vol. NS-32, n.5, p. 1933 (1985).
- [19] J. C. Sheppard et al., "Implementation of Nonintercepting Energy Spread Monitors", Proceedings of the IEEE Particle Accelerator Conference, Washington 1987 - IEEE Catalog No. 87CH2387-90, p.757, also SLAC Note SLAC-PUB-4101 (1986).

- [20] M. E. Biagini et al., "Observation of Ion Trapping at ADONE", Proceedings of the XIth International Conference on High Energy Accelerators, CERN - Geneva, July 1980, (Birkhäuser, Basle, 1980), p.687.
- [21] R. Bossart et al., "Proton Beam Profile Monitor Using Synchrotron Light", Proceedings of the XIth International Conference on High Energy Accelerators, CERN - Geneva, July 1980, (Birkhäuser, Basle, 1980), p.470.
- [22] D. A. Edwards, R. P. Johnson, F. Willeke, "Tests of Orbital Dynamics Using the Tevatron", Particle Accelerators, Vol. 19, No. 1-4, p.145 (1986).
- [23] A. Hofmann, "Dynamics of Beam Diagnostics", Lecture Notes - Academic Training Programme - CERN 1987 (unpublished).
- [24] A. Hofmann, "Diagnostics and Cures for Beam Instabilities", Proceedings of the XIth International Conference on High Energy Accelerators, CERN - Geneva, July 1980, (Birkhäuser, Basle, 1980), p.540 (1980).
- [25] A. Aragona et al., "Measurement and Steering of Beam Position in ADONE" - Nota Interna LNF 87/16 (P) (1987).
- [26] I. P. Karabekov, V. M. Tsakanov, "Coupling Coefficient and Tune Shift Measurements in High Energy Accelerators", Proceedings of the XIIth International Conference on High Energy Accelerators, Fermilab, August 1983, (FNAL, Batavia, Ill., 1983), p.220.